nature biotechnology

Chemical genetics screen for enhancers of rapamycin identifies a specific inhibitor of an SCF family E3 ubiquitin ligase

Mariam Aghajan[1,11], Nao Jonai[1,11], Karin Flick[2,11], Fei Fu[1], Manlin Luo[3], Xiaolu Cai[4], Ikram Ouni[2], Nathan Pierce[5], Xiaobo Tang[6], Brett Lomenick[1], Robert Damoiseaux[7], Rui Hao[1], Pierre M del Moral[8], Rati Verma[5], Ying Li[4], Cheng Li[9], Kendall N Houk[4], Michael E Jung[4], Ning Zheng[6], Lan Huang[10], Raymond J Deshaies[5], Peter Kaiser[2] & Jing Huang[1]

The target of rapamycin (TOR) plays a central role in eukaryotic cell growth control[1]. With prevalent hyperactivation of the mammalian TOR (mTOR) pathway in human cancers[2], strategies to enhance TOR pathway inhibition are needed. We used a yeast-based screen to identify small-molecule enhancers of rapamycin (SMERs) and discovered an inhibitor (SMER3) of the Skp1-Cullin-F-box (SCF)^{Met30} ubiquitin ligase, a member of the SCF E3-ligase family, which regulates diverse cellular processes including transcription, cell-cycle control and immune response[3]. We show here that SMER3 inhibits SCF^{Met30} *in vivo* and *in vitro*, but not the closely related SCF^{Cdc4}. Furthermore, we demonstrate that SMER3 diminishes binding of the F-box subunit Met30 to the SCF core complex *in vivo* and show evidence for SMER3 directly binding to Met30. Our results show that there is no fundamental barrier to obtaining specific inhibitors to modulate function of individual SCF complexes.

Conserved from yeast to humans, the target of rapamycin (TOR) protein is a serine/threonine protein kinase that controls various aspects of cellular growth by regulating translation, transcription, autophagy, cytoskeletal organization and metabolism[1]. Rapamycin, a secondary metabolite produced by *Streptomyces hygroscopicus*, specifically inhibits the activity of TOR, resulting in starvation-like phenotypes. Over the past few years, deregulation of pathways upstream and downstream of mTOR has been implicated in a variety of cancers, making the TOR signaling pathway a potential target for cancer therapy and rapamycin (and its analogs) an attractive anti-cancer agent[2]. Results from first-round clinical trials suggest that different types of tumors have different sensitivities to rapamycin and in many cases rapamycin does not completely halt the progress of the disease[4,5], thus making it desirable to identify small molecules that can act in concert with rapamycin. Although combination strategies taking advantage of known interacting pathways (e.g., mTOR and IGF1R, PI3K or AKT) are being pursued[6–8], an unbiased search for novel exploitable pathways has not been reported. The unbiased cell-based approach described here has the potential to elucidate new interactions of TOR signaling with other pathways and to provide valuable chemical tools to study signaling networks in various settings.

We and others have previously shown that yeast is a promising platform for high-throughput discovery of small-molecule modifiers of rapamycin-sensitive TOR functions, including both suppressors (small-molecule inhibitors of rapamycin or SMIRs) and enhancers (SMERs), which show potential for modulating TOR-related processes in higher organisms[9,10]. Here we used the yeast-based screen to identify new SMERs targeting cell growth control (Online Methods). Using a ChemBridge DiverSet library containing 30,000 small molecules, we identified >400 compounds that, in the presence of a suboptimal rapamycin concentration, gave a 'no growth' phenotype (**Supplementary Data Set 1**). After removing toxic compounds using unrelated screening data sets (Online Methods), a total of 86 potential SMERs were identified, which were synthetic sick/lethal with rapamycin but showed little toxicity by themselves at the concentrations used (**Supplementary Data Set 2** and **Supplementary Fig. 1**). The SMERs encompass a variety of modes of action and biological activities, including direct inhibition of mTOR kinase activity, new post-translational regulation of mTOR function, and inhibition of patient-derived brain tumor initiating cells (unpublished data). Five structurally distinct molecules that exhibited differing effects on growth (Online Methods) were selected for further analysis (**Fig. 1a**).

[1]Department of Molecular and Medical Pharmacology, David Geffen School of Medicine, and the Molecular Biology Institute, University of California, Los Angeles, California, USA. [2]Department of Biological Chemistry, School of Medicine, University of California, Irvine, California, USA. [3]Department of Biological Engineering, Massachusetts Institute of Technology, Cambridge, Massachusetts, USA. [4]Department of Chemistry and Biochemistry, University of California, Los Angeles, California, USA. [5]Department of Biology, Howard Hughes Medical Institute, California Institute of Technology, Pasadena, California, USA. [6]Department of Pharmacology, Howard Hughes Medical Institute, University of Washington, Seattle, Washington, USA. [7]Molecular Screening Shared Resource, University of California, Los Angeles, California, USA. [8]Roche Diagnostics Corporation, Roche Applied Science, Indianapolis, Indiana, USA. [9]Department of Biostatistics and Computational Biology, Dana-Farber Cancer Institute, Boston, Massachusetts, USA. [10]Departments of Physiology & Biophysics and Developmental & Cell Biology, University of California, Irvine, California, USA. [11]These authors contributed equally to this work. Correspondence should be addressed to J.H. (jinghuang@mednet.ucla.edu) or P.K. (pkaiser@uci.edu).

Received 9 March; accepted 9 May; published online 27 June 2010; doi:10.1038/nbt.1645

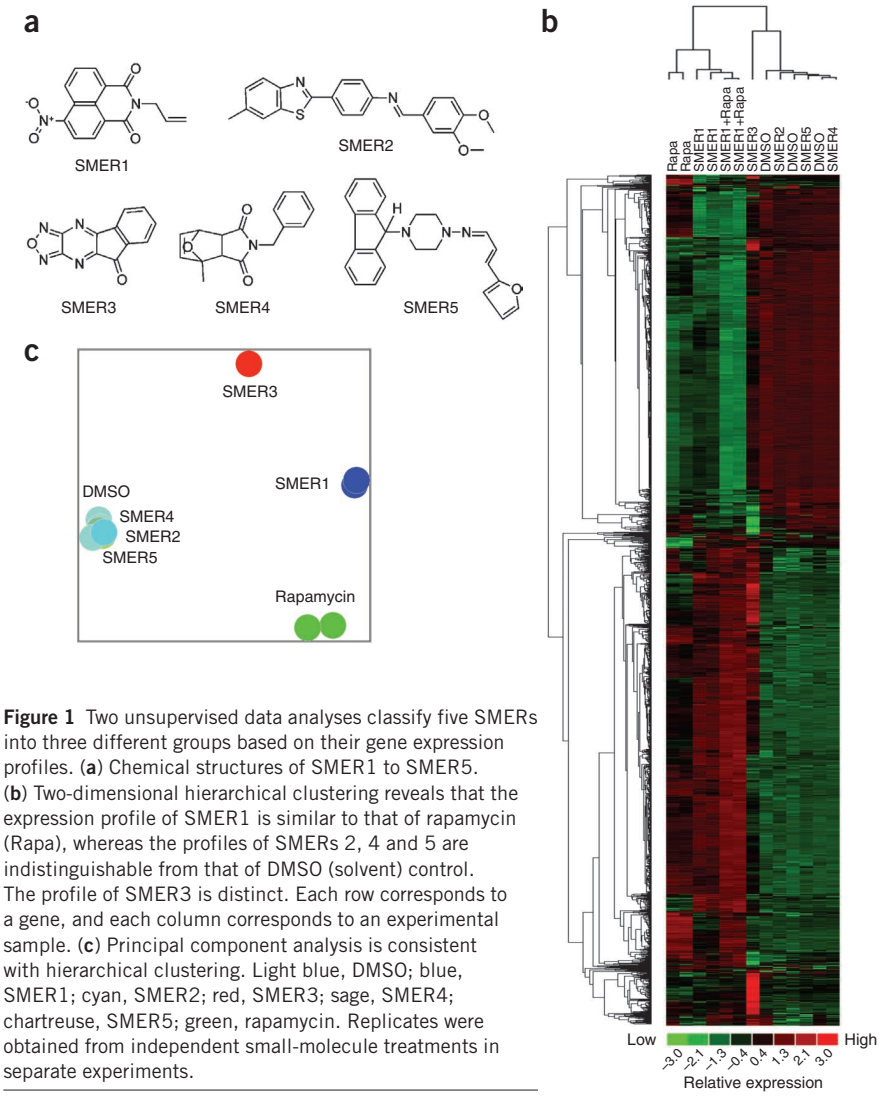

Figure 1 Two unsupervised data analyses classify five SMERs into three different groups based on their gene expression profiles. (**a**) Chemical structures of SMER1 to SMER5. (**b**) Two-dimensional hierarchical clustering reveals that the expression profile of SMER1 is similar to that of rapamycin (Rapa), whereas the profiles of SMERs 2, 4 and 5 are indistinguishable from that of DMSO (solvent) control. The profile of SMER3 is distinct. Each row corresponds to a gene, and each column corresponds to an experimental sample. (**c**) Principal component analysis is consistent with hierarchical clustering. Light blue, DMSO; blue, SMER1; cyan, SMER2; red, SMER3; sage, SMER4; chartreuse, SMER5; green, rapamycin. Replicates were obtained from independent small-molecule treatments in separate experiments.

The primary challenge for phenotype-based chemical genetic screens is the subsequent target identification, for which a variety of technologies—from affinity to genomics based—has been developed (see ref. 11 and reviews therein). We first sought to take advantage of the tremendous information on gene expression related to various cellular pathways in yeast and performed genome-wide expression profiling using DNA microarrays. We expected that expression profile changes induced by SMERs can be linked to gene expression changes caused by genetic perturbations[12]. To capture early and/or direct transcriptome changes and avoid secondary effects, cells were treated with SMERs for a short period (30 min) and the extracted RNA was processed to probe Affymetrix GeneChips (Online Methods).

The hierarchical clustering pattern of our microarray data classified the five SMERs identified from the screen into three distinct groups (**Fig. 1b**). Treatment of yeast cells with SMER2, 4 or 5 had no obvious effect on global gene transcription, whereas SMER1's effect on transcription shared extensive similarity with rapamycin (M.A., unpublished data). SMER3's expression profile, on the other hand, is different from all the others. Consistent with hierarchical clustering, principal components analysis (**Fig. 1c**) also readily distinguishes these effects on gene expression.

We focused primarily on SMER3, given its distinct profile. Notably, a set of methionine biosynthesis genes (referred to as *MET*-genes hereafter) was upregulated in SMER3-treated cells (**Supplementary Tables 1** and **2**). GO analysis revealed that, in addition to the enrichment of sulfur metabolism genes among the induced group, genes involved in cell-cycle regulation were overrepresented in the downregulated group of SMER3-specific genes (**Supplementary Tables 1** and **2**).

Induction of *MET*-gene expression in response to SMER3 exposure suggested that the cellular pathway controlling homeostasis of sulfur-containing compounds was a possible target for SMER3. The key regulator of this pathway is the ubiquitin ligase SCF^{Met30}, which restrains the transcriptional activator Met4 in an inactive state in a methionine-replete media by attachment of a regulatory ubiquitin chain[13]. Inactivation of SCF^{Met30} prevents Met4 ubiquitination, permitting the formation of an active Met4-containing transcription complex that induces expression of the *MET*-genes and blocks cell proliferation.

One hypothesis to explain the *MET*-gene activation and growth inhibition in SMER3-treated cells is that SMER3 inhibits SCF^{Met30}. In agreement with this notion, Met4 ubiquitination was blocked in cells exposed to SMER3 (but not to rapamycin) (**Fig. 2a**). Furthermore, genetic analyses have previously demonstrated that deubiquitinated Met4 mediates cell cycle arrest upon inactivation of SCF^{Met30} (ref. 13), and deletion of *MET4* rescues lethality of *met30Δ* (ref. 14). Notably, *met4*Δ cells were also less susceptible to growth inhibition by SMER3 (but not rapamycin, exemplifying specificity) (**Fig. 2b** and **Supplementary Fig. 2**). These findings are consistent with SMER3 being an inhibitor of SCF^{Met30}. However, the incomplete resistance of *met4*Δ to SMER3 (**Fig. 2b**) suggests that SMER3 likely has additional targets other than SCF^{Met30} and that cell growth inhibition by SMER3 is not solely due to SCF^{Met30} inhibition. This is not uncommon as even imatinib (Gleevec), which was originally believed to be a highly specific inhibitor of BCR-Abl, is now appreciated to exert its biological effects through protein kinases in addition to its intended target[15].

SMER3 enhances rapamycin's effect and also inhibits SCF^{Met30}, suggesting a connection between the TOR and SCF^{Met30} pathways. To test whether SMER3 functions as an enhancer of rapamycin through inhibition of SCF^{Met30}, we asked if genetic inhibition of SCF^{Met30} could mimic SMER3 in the synergistic effect with rapamycin. Indeed, hypomorphic alleles of the individual components of SCF^{Met30} and its E2 ubiquitin-conjugating enzyme, Cdc34, were hypersensitive to rapamycin (**Fig. 2c**). The synthetic lethality with rapamycin appears to arise largely from reduced SCF^{Met30} activity because inhibition of Cdc4, which forms a related, essential SCF^{Cdc4} ubiquitin ligase, only resulted in minor rapamycin hypersensitivity (**Fig. 2c**). Together these results suggest that SMER3 enhances rapamycin's growth inhibitory effect by inhibition of SCF^{Met30}.

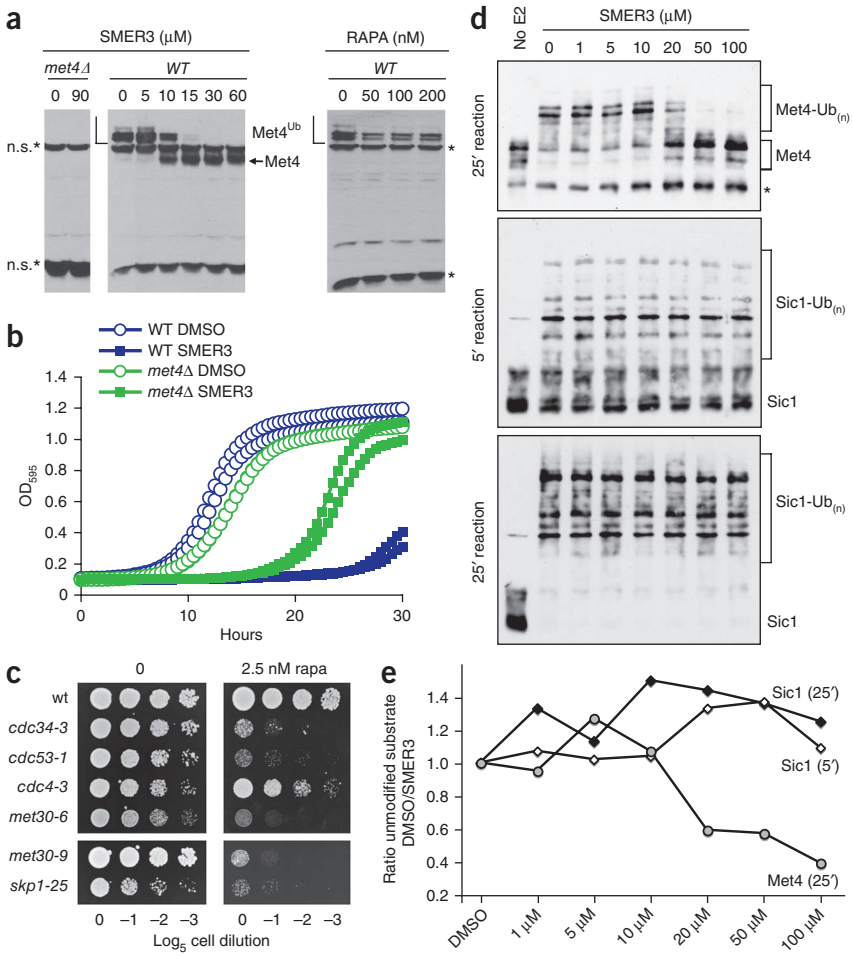

Figure 2 SMER3 targets SCF^{Met30}. (**a**) Biochemical evidence for SCF^{Met30} inhibition by SMER3 but not rapamycin. Yeast cells were cultured in YPDA medium to mid-log phase, treated with indicated concentrations of SMER3 or rapamycin for 45 min, and total protein was extracted for western blot analyses (Online Methods). Met4 ubiquitination *in vivo* can be directly assessed by immunoblotting because ubiquitinated forms of Met4 are not degraded by proteasomes and can thus be detected due to a characteristic mobility shift on denaturing gels[29]. The asterisks (*) denote nonspecific bands immunoreactive to the anti-Met4 antibody (generous gift from M. Tyers). (**b**) SMER3 resistance in *met4*Δ cells. Yeast cells were treated with either vehicle (DMSO) or 4 μM SMER3, and growth curve analysis was performed with an automated absorbance reader measuring O.D. at 595 nm every 30 min (Online Methods). Cell growth was measured in liquid because SMER3 activity is undetectable on agar. (**c**) Genetic interaction between SCF^{Met30} and TOR. Temperature-sensitive mutants as indicated were grown at 25 °C to mid-log phase in YPDA medium and serial dilutions were spotted onto plates with or without 2.5 nM rapamycin. The plates were incubated at the permissive temperatures for the mutants: 28 °C for *cdc34-3, cdc53-1, cdc4-3* and *met30-6* because these mutants exhibited fitness defects at 30 °C even without rapamycin, or 30 °C (standard growth temperature) for *met30-9* and *skp1-25* because these alleles are not temperature sensitive until 37 °C. (**d**) SMER3 specifically inhibits SCF^{Met30} E3 ligase *in vitro*. Components of SCF^{Met30} and SCF^{Cdc4} E3 ligases were expressed and purified from insect cells and used in *in vitro* ubiquitination assays. Reaction products were analyzed by immunoblotting. The asterisk indicates a protein cross-reacting with the anti-Met4 antibody. (**e**) The amount of unubiquitinated substrate (Met4 and Sic1) was quantified on a Fuji LAS-4000 imaging system, and inhibition was expressed as the ratio of unubiquitinated substrate in DMSO/SMER3.

To test whether SMER3 can directly inhibit SCF ubiquitin ligases, we assayed ubiquitination of well-established SCF substrates by purified SCF complexes *in vitro*. Indeed, addition of SMER3 to the ligase reactions inhibited ubiquitination of Met4 by SCF^{Met30} in a dose-dependent manner, whereas SMER1 had no effect (**Supplementary Fig. 3**). To assess specificity of SMER3, we also examined *in vitro* ubiquitination of Sic1 by the related WD40 repeat containing SCF^{Cdc4}. For direct comparison of SMER3's effects, activities of SCF^{Met30} and SCF^{Cdc4} were analyzed in a single reaction mix containing both ligase complexes and their substrates Met4 and Sic1 (**Fig. 2d**). Owing to the faster kinetics of the SCF^{Cdc4}-catalyzed ubiquitination, the Sic1 reaction was probed at two incubation times: first at 5 min, corresponding to the linear range for the SCF^{Cdc4} reaction (at which time there was no Met4 ubiquitination by SCF^{Met30}), then at 25 min, corresponding to the linear range of the SCF^{Met30} reaction. Consistent with the selective *in vivo* effect of SMER3 on SCF^{Met30}, *in vitro* ubiquitination of Sic1 was unaffected by SMER3 (**Fig. 2d**,**e**). In some experiments with SCF^{Cdc4}, a modest effect is seen on high molecular weight conjugates (data not shown), but it is clear from the direct head-to-head comparison where both enzymes are in the same tube that there is a very large difference in sensitivity of the two ligase complexes toward SMER3.

To investigate the mechanisms of specificity in the inhibition of SCF^{Met30} by SMER3, we examined the association of Met30 and the SCF core component Skp1. We found that Met30 was no longer bound to Skp1 immunopurified from cells treated with SMER3 (**Fig. 3a**), suggesting that SMER3 prevents the assembly of SCF^{Met30} or induces SCF complex dissociation (**Supplementary Note**). We next asked whether SMER3 affects the binding of other Skp1 interactors or acts specifically on SCF^{Met30}. Skp1-bound proteins were purified from cells treated with SMER3 or DMSO solvent control and their relative abundance was determined using stable isotope labeling with amino acids in cell culture (SILAC)-based quantitative mass spectrometry. Among the 11 identified F-box proteins, only binding of Met30 to Skp1 was substantially inhibited by SMER3 (**Fig. 3b**). Skp1 and Met30 protein levels were not affected by SMER3, nor were the interactions of the SCF core components Cdc53 (cullin) and Hrt1 (RING component) with Skp1 (**Fig. 3b** and **Supplementary Fig. 4**).

To further address the specificity of SMER3 for Met30 *in vivo*, we compared the cell cycle arrest phenotype induced by SMER3 to that of temperature-sensitive mutants of Met30, Cdc4 and the SCF components induced by nonpermissive temperatures. SMER3 induces a phenotype resembling that of genetic inhibition of Met30, whereas genetic inhibition of general SCF components or the specific F-box subunit Cdc4 gives a completely different elongated cell cycle arrest phenotype (**Fig. 3c**). Inhibition of any of the SCF core components simultaneously blocks SCF^{Met30} and SCF^{Cdc4}, yet the arrest phenotypes

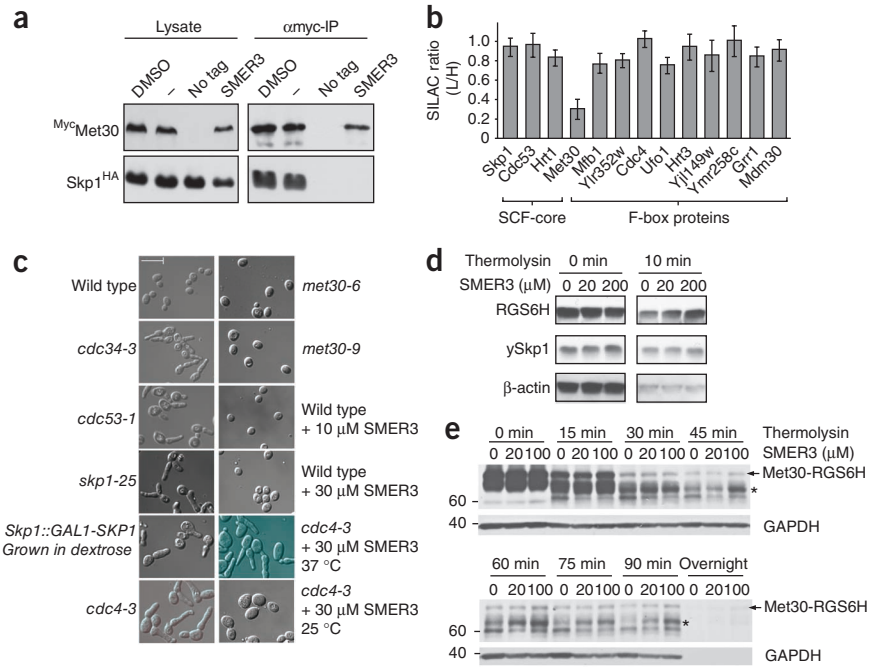

Figure 3 Molecular mechanism for the specificity of SCF^{Met30} inhibition by SMER3. (**a**) Protein-protein interaction between Met30 and Skp1 is diminished by SMER3 *in vivo*. Yeast cells expressing endogenous 13Myc-tagged Met30 were either untreated, or treated with solvent control (DMSO) or 30 μM SMER3 for 30 min at 30 °C. ^{13Myc}Met30 was immunopurified and immunocomplexes were analyzed for Skp1 binding by western blot analysis. (**b**) SMER3 specifically targets SCF^{Met30} *in vivo* as determined by quantitative mass spectrometry. A yeast strain expressing endogenous HBTH-tagged Skp1 was grown in medium containing either heavy ($^{13}C/^{15}N$) or light ($^{12}C/^{14}N$) arginine and lysine to metabolically label proteins. Skp1-bound proteins were purified and analyzed by mass spectrometry. Abundance ratios for SCF components identified by multiple quantifiable peptides are shown as SILAC ratios of 'light' (SMER3-treated) over 'heavy' (DMSO-treated) peptide intensities. (**c**) SMER3 specificity for SCF^{Met30} versus SCF^{Cdc4} as verified by cell cycle arrest morphology. Temperature-sensitive mutants were shifted to 37 °C for 4 h. The Skp1 depletion phenotype was observed after repression of Skp1 expression in dextrose medium for 12 h. SMER3 treatment of cells was for 6 h. Scale bar, 10 μm. (**d**) SMER3 protects endogenous Met30 from protease digestion. Yeast cells expressing Met30-RGS6H were lysed and digested with thermolysin in the presence of SMER3 versus DMSO control, and the extent of proteolysis was analyzed by immunoblotting. (**e**) SMER3 protects recombinant Met30 from protease digestion. The asterisks (*) indicate the Met30 fragment that is protected by SMER3 from protease digestion. Full-length blots for **a**,**d** and **e** are in **Supplementary Figure 8**.

of SCF core mutants strongly resemble Cdc4 inhibition (**Fig. 3c**). This indicates that the *cdc4* cell cycle arrest morphology is 'dominant' over that of *met30* and that inhibition by SMER3 is indeed specific for Met30 without affecting Cdc4 or SCF in general. Additionally, whereas SMER3-treated *cdc4* temperature-sensitive mutant cells have a phenotype at permissive temperatures resembling genetic inhibition of Met30, their phenotype changes to that resembling Cdc4 inhibition when shifted to nonpermissive temperatures (**Fig. 3c**), further demonstrating that SMER3 has little effect on Cdc4 *in vivo*.

To test direct binding of SMER3, we employed differential scanning fluorimetry[16] using purified Met30-Skp1 versus Skp1 proteins (Met30 cannot be obtained in isolation without Skp1). The addition of SMER3 altered the melting temperature of Met30-Skp1, but not that of Skp1 alone, indicating that SMER3 does indeed directly target the Met30-Skp1 complex (**Table 1**). The simplest model to explain the biochemical specificities of SMER3 is that it binds directly to Met30 but not Skp1. Because drug binding often stabilizes a folded state or conformation of its protein target, leading to increased resistance to protease digestion (as assayed by drug affinity responsive target stability or DARTS[11]), we tested whether protease susceptibility of Met30 is altered by the presence of SMER3. Indeed, when yeast cell lysates were treated with the protease thermolysin, we observed SMER3-dependent protection of Met30 (**Fig. 3d**,**e** and **Supplementary Fig. 5**), but not Skp1. These experiments suggest that Met30 is the direct molecular target of SMER3, although we cannot exclude that SMER3 binding to Met30 may require Skp1.

Met30 contains at its N terminus the F-box motif, which binds Skp1, and at the C terminus the WD40 repeats, which serve as protein-protein interaction motifs for substrate binding[17]. We found that the Met30 F-box, but not the Cdc4 F-box, was protected to a similar extent as full-length Met30 by the presence of SMER3 in DARTS experiments (**Supplementary Figs. 6** and **7**). In contrast, SMER3 failed to protect the WD40 repeat domain of Met30 (**Supplementary Fig. 6** and **Supplementary Note**). These results suggest that SMER3 may recognize the F-box motif of Met30, yet further investigation is required to understand how SMER3 binds to Met30.

In this study, we demonstrated that SMER3 (i) specifically inhibits *in vitro* ubiquitination by recombinant reconstituted SCF^{Met30} (**Fig. 2d**,**e** and **Supplementary Fig. 3**), (ii) selectively disassembles or prevents assembly of SCF^{Met30} but not other SCF complexes *in vivo* (**Fig. 3a–c**) and (iii) directly binds to Met30 (or Met30-Skp1 complex), but not Skp1 alone (**Fig. 3d** and **Table 1**). Together, these experiments suggest that SMER3 specifically inactivates SCF^{Met30} by binding to Met30.

Designing specific inhibitors for SCFs has historically been considered highly challenging owing to their common scaffolding subunits and similar enzymatic steps[18–21], reminiscent of the obstacles faced with kinase inhibitors[22]. The biological specificities demonstrated by this first-generation hit provide encouraging examples for

Table 1 SMER3 binding to Met30-Skp1 in DSF

	Tm (°C)		
	Met30 (2 μM)	Met30 (4 μM)	Skp1 (5 μM)
DMSO	45.17	48.03	45.65
1 μM SMER3	46.00	48.02	46.17
10 μM SMER3	27.85	26.90	46.42
100 μM SMER3	27.13	26.45	45.02
1 μM Rapamycin	46.30		46.08
10 μM Rapamycin		47.70	45.98

SMER3 directly binds to Met30-Skp1, but not Skp1 alone, as determined by differential scanning fluorimetry (DSF). Met30 and Skp1 were either co-expressed or Skp1 was expressed alone in insect cells and the complex was purified based on a GST-tag fused to Met30, whereas Skp1 was purified based on a His-tag fused to Skp1. Protein, drug and Sypro Orange dye were added to 384-well plates and melting curve fluorescent signal was detected using the LightCycler 480 System II. Melting temperatures (Tm) were determined by the LightCycler 480 Protein Melt Analysis Tool.

such potential and highlight the importance of unbiased cell-based approaches in drug discovery and in biological studies.

In conclusion, we identified several small-molecule enhancers of rapamycin from a phenotype-based chemical genetic screen. Genomic, genetic and biochemical analyses indicate that one of the SMERs (SMER3) inhibits an E3 ubiquitin ligase in yeast, SCF^{Met30}, which coordinates nutritional responses with cell proliferation. Because increasing evidence suggests that ubiquitin E3 ligases are involved in tumorigenesis[23], we believe that SMER3 and SMER3-like molecules represent a class of E3 ubiquitin ligase inhibitors that can potentially be used as anti-cancer drugs in the future.

In addition, our study provides a link between the TOR pathway and a separate network that monitors the sulfur-containing amino acids methionine, cysteine and the primary methyl group donor S-adenosylmethionine (SAM). This genetic interaction may be simply explained by the convergence of these two pathways on regulation of the G1 cyclins (refs. 14,24 and see **Supplementary Table 2** for SMER3). Alternatively, it is possible that more complicated co-regulations occur in which TOR inhibition, although insufficient for activation of the 'sulfur starvation' response, may in fact enhance this response during times of sulfur depletion (**Supplementary Note**). We have preliminary data suggesting that SMER3 also acts in a synthetic lethal fashion with rapamycin in human A549 lung cancer cells (data not shown), but the target pathway for SMER3 in mammalian cells has yet to be determined. It is noteworthy that cancer cells and tumors are particularly dependent on metabolic networks linked to methionine[25,26], indicating that mammalian processes similar to that controlled by SCF^{Met30} in yeast might provide potential anti-cancer targets.

Synthetic lethal interactions between rapamycin and the ubiquitin-like modification systems (**Fig. 2c**) suggest potential therapeutic benefit for combination therapy with rapamycin and any small molecule that inhibits a component of SCF or an activator of SCF, such as in sensitizing a tumor's response to rapamycin and/or preempting the development of drug resistance. Beyond cancer and tumor-prone syndromes, a variety of other diseases including hypertrophy, neurodegeneration and aging are linked to the TOR pathway[27,28]. For example, several SMERs have been identified that effectively enhance autophagy and reduce toxicity in Huntington's disease models through unknown mechanisms[10]. Similar chemical genetic approaches are applicable to the study of other pathways, drugs and diseases.

METHODS

Methods and any associated references are available in the online version of the paper at http://www.nature.com/naturebiotechnology/.

Accession codes. NCBI Gene Expression Omnibus (GEO), GSE22269. The library database and complete genomic data sets are also available on the web (http://labs.pharmacology.ucla.edu/huanglab).

Note: Supplementary information is available on the Nature Biotechnology website.

ACKNOWLEDGMENTS

We are grateful for grant support from the American Cancer Society and the U.S. National Institutes of Health and for traineeship support of M.A. and B.L. by the NIH UCLA Chemistry–Biology Interface Predoctoral Training Program. N.Z. and R.J.D. are investigators of the Howard Hughes Medical Institute. We thank D. Skowyra (Saint Louis University) and M. Tyers (University of Edinburgh, UK) for their generous gifts of bacculo virus constructs and anti-Met4 antibody, respectively. We also thank J. Salcedo (Roche Diagnostics Corporation) for support toward differential scanning fluorimetry experiments.

AUTHOR CONTRIBUTIONS

Figure 1a, M.A. and R.D.; **1b**, F.F. and M.L.; **1c**, C.L. and J.H.; **2a**, N.J.; **2b**, N.J. and R.H.; **2c**, K.F.; **2d,e**, I.O. and N.P.; **3a**, K.F.; **3b**, K.F. and L.H.; **3c**, K.F.; **3d**, N.J.; **3e**, M.A.; **Table 1**, X.T., M.A. and P.M.d.M.; X.C., B.L., R.V., Y.L., K.N.H., M.E.J. and N.Z. contributed new reagents and analysis; all authors discussed data; M.A., F.F., M.E.J., R.J.D., P.K. and J.H. wrote the paper with input from all authors.

COMPETING FINANCIAL INTERESTS

The authors declare no competing financial interests.

Published online at http://www.nature.com/naturebiotechnology/.
Reprints and permissions information is available online at http://npg.nature.com/reprintsandpermissions/.

1. Wullschleger, S., Loewith, R. & Hall, M.N. TOR signaling in growth and metabolism. *Cell* **124**, 471–484 (2006).
2. Bjornsti, M.A. & Houghton, P.J. The TOR pathway: a target for cancer therapy. *Nat. Rev. Cancer* **4**, 335–348 (2004).
3. Petroski, M.D. & Deshaies, R.J. Function and regulation of cullin-RING ubiquitin ligases. *Natl. Rev.* **6**, 9–20 (2005).
4. Easton, J.B. & Houghton, P.J. mTOR and cancer therapy. *Oncogene* **25**, 6436–6446 (2006).
5. Cloughesy, T.F. *et al.* Antitumor activity of rapamycin in a Phase I trial for patients with recurrent PTEN-deficient glioblastoma. *PLoS Med.* **5**, e8 (2008).
6. Chiang, G.G. & Abraham, R.T. Targeting the mTOR signaling network in cancer. *Trends Mol. Med.* **13**, 433–442 (2007).
7. Shaw, R.J. & Cantley, L.C. Ras, PI(3)K and mTOR signalling controls tumour cell growth. *Nature* **441**, 424–430 (2006).
8. Guertin, D.A. & Sabatini, D.M. Defining the role of mTOR in cancer. *Cancer Cell* **12**, 9–22 (2007).
9. Huang, J. *et al.* Finding new components of the target of rapamycin (TOR) signaling network through chemical genetics and proteome chips. *Proc. Natl. Acad. Sci. USA* **101**, 16594–16599 (2004).
10. Sarkar, S. *et al.* Small molecules enhance autophagy and reduce toxicity in Huntington's disease models. *Nat. Chem. Biol.* **3**, 331–338 (2007).
11. Lomenick, B. *et al.* Target identification using drug affinity responsive target stability (DARTS). *Proc. Natl. Acad. Sci. USA* (in the press) (2009).
12. Hughes, T.R. *et al.* Functional discovery via a compendium of expression profiles. *Cell* **102**, 109–126 (2000).
13. Kaiser, P., Su, N.Y., Yen, J.L., Ouni, I. & Flick, K. The yeast ubiquitin ligase SCFMet30: connecting environmental and intracellular conditions to cell division. *Cell Div.* **1**, 16 (2006).
14. Patton, E.E. *et al.* SCF(Met30)-mediated control of the transcriptional activator Met4 is required for the G(1)-S transition. *EMBO J.* **19**, 1613–1624 (2000).
15. Sawyers, C.L. Imatinib GIST keeps finding new indications: successful treatment of dermatofibrosarcoma protuberans by targeted inhibition of the platelet-derived growth factor receptor. *J. Clin. Oncol.* **20**, 3568–3569 (2002).
16. Niesen, F.H., Berglund, H. & Vedadi, M. The use of differential scanning fluorimetry to detect ligand interactions that promote protein stability. *Nat. Protoc.* **2**, 2212–2221 (2007).
17. Bai, C. *et al.* SKP1 connects cell cycle regulators to the ubiquitin proteolysis machinery through a novel motif, the F-box. *Cell* **86**, 263–274 (1996).
18. Zheng, N. *et al.* Structure of the Cul1-Rbx1-Skp1-F boxSkp2 SCF ubiquitin ligase complex. *Nature* **416**, 703–709 (2002).
19. Chen, Q. *et al.* Targeting the p27 E3 ligase SCF(Skp2) results in p27- and Skp2-mediated cell-cycle arrest and activation of autophagy. *Blood* **111**, 4690–4699 (2008).
20. Nakajima, H., Fujiwara, H., Furuichi, Y., Tanaka, K. & Shimbara, N. A novel small-molecule inhibitor of NF-kappaB signaling. *Biochem. Biophys. Res. Commun.* **368**, 1007–1013 (2008).
21. Soucy, T.A. *et al.* An inhibitor of NEDD8-activating enzyme as a new approach to treat cancer. *Nature* **458**, 732–736 (2009).
22. Knight, Z.A. & Shokat, K.M. Features of selective kinase inhibitors. *Chem. Biol.* **12**, 621–637 (2005).
23. Nalepa, G., Rolfe, M. & Harper, J.W. Drug discovery in the ubiquitin-proteasome system. *Nat. Rev. Drug Discov.* **5**, 596–613 (2006).
24. Zinzalla, V., Graziola, M., Mastriani, A., Vanoni, M. & Alberghina, L. Rapamycin-mediated G1 arrest involves regulation of the Cdk inhibitor Sic1 in *Saccharomyces cerevisiae*. *Mol. Microbiol.* **63**, 1482–1494 (2007).
25. Halpern, B.C., Clark, B.R., Hardy, D.N., Halpern, R.M. & Smith, R.A. The effect of replacement of methionine by homocystine on survival of malignant and normal adult mammalian cells in culture. *Proc. Natl. Acad. Sci. USA* **71**, 1133–1136 (1974).
26. Guo, H. *et al.* Therapeutic tumor-specific cell cycle block induced by methionine starvation in vivo. *Cancer Res.* **53**, 5676–5679 (1993).
27. Lee, C.H., Inoki, K. & Guan, K.L. mTOR pathway as a target in tissue hypertrophy. *Annu. Rev. Pharmacol. Toxicol.* **47**, 443–467 (2007).
28. Harrison, D.E. *et al.* Rapamycin fed late in life extends lifespan in genetically heterogeneous mice. *Nature* **460**, 392–395 (2009).
29. Flick, K. *et al.* Proteolysis-independent regulation of the transcription factor Met4 by a single Lys 48-linked ubiquitin chain. *Nat. Cell Biol.* **6**, 634–641 (2004).

ONLINE METHODS

Chemical genetic screen. The screen for SMERs was carried out as described[9] with several modifications. The earlier screen, using a high rapamycin concentration, was designed to identify potent SMIR activities. Here, the following modifications were made to optimize the identification of SMERs: (i) lowering the concentration of rapamycin such that it inhibits wild-type yeast only partially, thereby facilitating the detection of synthetic lethal hits, and (ii) raising the final concentrations of library compounds in the medium (2.5×; ~25 μM) to better recognize (and eliminate) hits that are cytotoxic even without rapamycin. Other changes include the use of a larger collection of the ChemBridge DiverSet library and implementation of robotic pin transfer to deliver library compounds. The library database is available on our web site (http://labs.pharmacology.ucla.edu/huanglab/).

Selection of SMERs. Yeast growth was scored using a scale of "1–" (least) to "6–" (most severe growth inhibition) by visual inspection once a day for 5 d, resulting in 446 compounds that caused varying degrees of 'no growth' phenotype. Growth results were compared to OD data obtained from an unrelated screen[30] performed with the same compound library to eliminate potential nonspecific toxic hits. This was done by categorizing compounds as corresponding to growth that is at least 1 s.d. below the average OD reading, at least 1 s.d. above the average reading, and no significant change. If a compound was seen to significantly inhibit growth in this unrelated screen and our screen, it was eliminated as a nonspecific toxic hit, narrowing the list of 446 hits to 86 compounds (SMERs). Further, the SMERs were sorted based on the OD readings from the unrelated screen, followed by sorting based on our own growth rankings, allowing for growth comparison between both screens owing to compound treatment. SMERs 1, 3 and 4 were selected based on their ability to severely inhibit growth in our screen (6– score), while exhibiting no effects on growth in unrelated screens. SMERs 2 and 5, on the other hand, only weakly affected growth in our screen (2– score) and displayed no effects on growth in unrelated screens. By selecting structurally distinct compounds that exhibit differing degrees of growth inhibition, we hoped to isolate SMERs that have different cellular targets and/or mechanisms of action.

Expression analysis (experimental part). Yeast cells were grown to mid-log phase (0.5–2 × 10^7 cells/ml) at 30 °C, in YPD medium, unless otherwise specified, before treatment with small molecules for 30 min. Treated cells were harvested and flash frozen in liquid nitrogen. Total RNA was isolated using the RiboPure Yeast kit (Ambion) and RNA quality was checked using an Agilent 2100 Bioanalyzer (Agilent Technologies). Biotin-labeled cRNA probes were generated from total RNA using the One-Cycle Target Labeling Assay and used for hybridization to Affymetrix GeneChip Yeast Genome 2.0 arrays (Affymetrix), according to manufacturer's specifications. The Yeast 2.0 array includes ~5,744 probe sets for 5,841 of the 5,845 genes present in *S. cerevisiae* and 5,021 probe sets for all 5,031 genes present in *S. pombe*. The arrays were scanned using Affymetrix GeneChip Scanner 3000 (Affymetrix) and raw data generated using the GeneChip Operating System GCOSv1.4. Raw data were further processed and analyzed using GCOS or dChip (see below) as indicated.

Gene expression analysis (computational part). Gene expression data were normalized in dChip (http://www.dchip.org/)[31]. Model-based expression indices were calculated and log2 transformed. Genes were filtered by two criteria: the s.d. across the samples had to be between 0.5 and 1,000, and the genes had to be present in at least 20% of the samples. Hierarchical clustering and principal component analysis on filtered genes were performed in dChip. Differentially expressed genes were selected by the following criteria: there should at least be a twofold difference in expression between treatments and controls; the *P*-value of the two-tailed, two-sample unpaired equal variance *t*-test must be <0.05. GO (gene ontology)[32] analysis was performed using GO term finder on the *Saccharomyces* Genome Database (http://www.yeastgenome.org/). The complete data sets are available on the web (http://labs.pharmacology.ucla.edu/huanglab/).

Protein analyses. Yeast cells were cultured to mid-log phase (~0.8 × 10^7 cells/ml) at 30 °C, in YPD medium, or YPD plus adenine (YPDA) medium where indicated, for small-molecule treatment. Equal concentration of DMSO carrier (0.45% here) was used across all samples. For western blot analysis, protein extracts were prepared in 8 M urea buffer (8 M urea, 0.2% SDS, 200 mM NaCl, 100 mM Tris-HCl pH 7.5, phosphatase inhibitors (10 mM sodium pyrophosphate, 5 mM EDTA, 5 mM EGTA, 50 mM NaF, and 0.1 mM orthovanadate), and complete protease inhibitor cocktail (Roche)). Cell pellets were broken with glass beads for 2 × 40 s at 4 °C in a FastPrep-24 (MP Biomedicals). Whole cell lysates were collected after centrifugation (18,000*g*, 10 min) and diluted to a final concentration of 4 M urea for SDS-PAGE. Proteins were transferred to a PVDF membrane and probed with antibodies as indicated.

For immunoprecipitation cells were lysed in (50 mM HEPES pH 7.5, 0.2% Triton X-100, 200 mM NaCl, 10% glycerol, 1 mM DTT, 10 mM Na-pyrophosphate, 5 mM EDTA, 5 mM EGTA, 50 mM NaF, 0.1 mM orthovanadate, 1 mM PMSF, and 1 μg/ml each aprotinin, leupeptin and pepstatin). Protein complexes were immunopurified with anti-myc antibodies (Santa Cruz Biotechnology), washed three times with 1 ml lysis buffer, and proteins were eluted by boiling in SDS-PAGE loading buffer before analysis by immunoblotting.

Generation of the *met4* null strain. The *met4*Δ strain was generated in the BY4741 strain background via one-step replacement of the MET4 open reading frame with a kanMX6 cassette[33] and selected for YPD/G418 plates supplemented with 20 μM S-adenosylmethionine (SAM, which is required for viability of the *met4Δ* mutant in this background). All deletions were verified with PCR. Primer sequences used are shown below.

MET4-F1:
5′-aagcgcacttctgataagcacttttattccttttttccactgtgaacgcggatccccgggttaattaa-3′
MET4-R1:
5′-tgcacgtatatatatatatatatatatattaaactgtatagtctgttattgaattcgagctcgtttaaac-3′
MET4-C1:
5′-ctcgtcgcacatgctattgt-3′
MET4-C2:
5′-ccacgtaggccaactgttct-3′
Kan_755R:
5′- atacctggaatgctgttttgccgg-3′

Growth curve analysis. Wild-type or *met4*Δ yeast cells in the BY4741 background were seeded in a 96-well plate format at an initial cell density of 2 × 10^5 cells/ml in YPD + SAM (50 μM), in the presence of SMER3, rapamycin, or DMSO carrier control. Plates were incubated, without shaking, at 30 °C and automated absorbance (optical density or O.D.) measurements of each culture well were taken at 595 nm every 30 min for 30 h using SpectraMax 340PC microplate reader (Molecular Devices).

Synthesis of 9*H*-Indeno[2,1-*b*][1,2,5]oxadiazolo[3,4-*e*]pyrazin-9-one, SMER3. To a stirred solution of 3,4-diaminofurazan (100 mg, 1.0 mmol) in acetic acid (2.5 ml) and ethanol (2.5 ml) was added ninhydrin (178 mg, 1.0 mol). The mixture was stirred at reflux overnight and cooled to 22 °C. The precipitate was collected by filtration, washed with ethanol (20 ml) and dried to give the product (SMER3, 198 mg, 88%) as a yellow solid. 1H NMR (400 MHz, DMSO-d_6) δ 8.29 (m, 1H), 8.05 (m, 2H), 7.95 (t, J = 6.8 Hz, 1H).

SCF E3 ligase assay. Met4 *in vitro* ubiquitination assays were carried out as previously described[34] with the exception that recombinant SCF^{Met30} components and $^{FLAG\text{-}6xHis}$Met4 were expressed in Hi5 cells. Briefly, ^{Gst}Skp1, Cdc53, ^{6xHis}Met30 and Rbx1 were co-expressed in Hi5 cells and SCF^{Met30} was purified on glutathione sepharose. Recombinant $^{FLAG\text{-}6xHis}$Met4 was bound to SCF^{Met30} and the ligase/substrate complex was eluted with glutathione. Sic1 *in vitro* ubiquitination by recombinant SCF^{Cdc4} was performed as described[35], with the exception that ubiquitinated Sic1 was detected by immunoblotting. To directly compare the effect of SMER3 on SCF^{Met30} and SCF^{Cdc4}, Met4 and Sic1 ubiquitination were assayed in a single reaction. Approximately 150 nM SCF^{Met30} and SCF^{Cdc4} were incubated with DMSO (solvent control) or SMER3 for 20 min at 25 °C. The reaction was started by addition of a final concentration of 250 nM yeast E1 (Boston Biochem), 0.8 μM recombinant

Cdc34 purified from *E. coli*[36], 5 mM ATP, and 80 µM ubiquitin (Sigma). Reactions were incubated at 30 °C and samples were taken after 5 min and 25 min reaction time to accommodate different reaction kinetics by the two SCFs. Products were separated on SDS-PAGE and analyzed by immunoblotting using anti-Met4 and anti-Sic1 antibodies. Quantification was done on a Fuji LAS-4000 imaging system.

Quantitative comparison of Skp1 complexes after SMER3 treatment by mass spectrometry. A yeast strain expressing N-terminal HBTH-tagged Skp1 from the endogenous locus was generated by a PCR-based approach as described[37]. Briefly, a PCR-based integration of a *TRP1-GAL1-HBTH* was used to generate a strain expressing HBTH-tagged Skp1. This strain is viable only on galactose plates. A PCR fragment encoding the SKP1 promoter with flanking homology regions for the HBTH tag and 5′ regions of the SKP1 gene was then used to replace the *TRP1-GAL1* fragment at the *SKP1* locus. Transformants were selected for growth on dextrose plates. The resulting strain carried the HBTH-tag inserted into the *SKP1* locus before the coding region without any other changes at the locus.

To quantitatively analyze changes in Skp1-associated proteins in response to SMER3, we used the QTAX strategy[38]. Briefly, for SILAC labeling, 200 ml cultures of cells expressing ^{HBTH}Skp1 were grown in medium containing either 30 mg/l ^{12}C ^{14}N arginine and 100 mg/l lysine ('light') or the same amount of $^{13}C_6$ $^{15}N_4$ arginine (isotopic purity > 98 atom %) and $^{13}C_6$ $^{15}N_2$ lysine (isotopic purity > 98 atom %) (Cambridge Isotope Labeling) ('heavy'). When cells reached an A_{600} of 0.5, the light culture was treated with 20 µM SMER3 for 30 min at 30 °C. The same amount of DMSO was added to the heavy culture as solvent control. Formaldehyde was then added to both cultures to a final concentration of 1% to cross-link and stabilize protein complexes *in vivo*, and cells were incubated at 30 °C for 10 min. Cross-linking was quenched by the addition of 125 mM glycine for 5 min at 30 °C. Cells were harvested by filtration and stored at –80 °C.

Cell lysis and purification of proteins was performed as described[38,39] with the following modifications. Cells were lysed with glass beads in 500 µl of buffer-1 (8 M urea, 300 mM NaCl, 0.5% Nonidet P-40, 50 mM sodium phosphate, 50 mM Tris, pH 8, 20mM imidazole) per tube in a FastPrep FP120 system. Cleared lysates were pooled and 10 mg of total protein extract of each light and heavy lysate were mixed and then incubated with Ni2+-sepharose (pre-equilibrated in buffer-1) (Amersham Biosciences) overnight at 25 °C. Ni^{2+}-sepharose was then washed once in buffer-1 and twice in buffer-1, pH 6.3. Proteins were eluted in buffer-2 (8 M urea, 200 mM NaCl, 50 mM sodium phosphate, 2% SDS, 10 mM EDTA, 100 mM Tris, pH 4.3). The pH of the eluate was adjusted to pH 8.0, and then loaded onto immobilized streptavidin (pre-equilibrated in buffer-3 (8 M urea, 200 mM NaCl, 0.2% SDS, 100 mM Tris, pH 8.0)) (Pierce). After incubation for 5 h at 25 °C the streptavidin beads were washed three times in buffer-3, and three times in buffer-3 without SDS. Streptavidin beads were then washed extensively with 25 mM NH_4HCO_3, pH 8, and the proteins were released by on-bead digestion with trypsin at 37 °C for 12–16 h. Tryptic peptides were extracted three times using 25% (vol/vol) acetonitrile, 0.1% (vol/vol) formic acid. The peptides were further purified on Vivapure C18 micro spin columns according to the manufacturer's instructions (Sartorius Biotech). Peptides were analyzed by 1D LC-MS/MS using a nanoLC system (Eksigent) coupled online to a Linear Ion Trap (LTQ)-Orbitrap XL mass spectrometer (Thermo-Electron) as described[40]. Data were analyzed using Protein Prospector developmental version 5.1.7. Relative abundance of proteins was determined by measuring the peptide peak intensities.

DARTS experiment using recombinant Met30. Met30 was PCR-subcloned into pcDNA3.1(-) (Invitrogen) and expressed using Promega TnT T7 Quick Coupled Transcription/Translation System. Thermolysin digestion was performed using translated lysate incubated with SMER3 or vehicle control, and stopped by adding EDTA pH 8.0. Samples were subjected to 4 -12% NuPAGE gradient gel (Invitrogen) and western blot analysis carried out with anti-RGSH (Qiagen) and anti-GAPDH (Ambion) antibodies.

Protein expression and purification. Full-length Met30 and Skp1 (yeast) proteins were overexpressed in insect cells as a glutathione S-transferase (GST)-fusion protein and N-terminal 6X His-tagged protein, respectively. After co-infection with both viruses expressing GST-Met30 and His-Skp1, GST-Met30 and His-Skp1 complex was isolated from the soluble cell lysate by glutathione affinity chromatography. The Met30/Skp1 protein complex was released from the column after cleavage by TEV protease. The protein sample was in a final solution of 20 mM Tris-HCl (pH 8.0), 200 mM NaCl and 5 mM DTT.

Full-length yeast Skp1 (N-terminal 6X His-tagged protein, as above) was overexpressed in insect cells and isolated from the soluble cell lysate using Ni-NTA affinity chromatography. The protein sample was in a final solution of 20 mM Tris-HCl, 300 mM NaCl and 15 mM imidazole.

Differential scanning fluorimetry. Protein melting experiments were carried out using the LightCycler 480 System II (Roche). Protein melting was monitored measuring the fluorescence of the hydrophobic dye Sypro Orange (Invitrogen) binding to amino acids of a denatured protein. The instrument was set up with a detection format of 465 nm as the excitation wavelength and 580 nm as the emission wavelength to detect Sypro Orange–specific signal. Melting curve fluorescent signal was acquired between 20 °C and 85 °C using a ramping rate of 0.06 °C s^{-1}, and an acquisition of ten data points per degree Celsius. Melting temperatures (Tm) were determined by the LightCycler 480 Protein Melt Analysis Tool.

30. Duncan, M.C., Ho, D.G., Huang, J., Jung, M.E. & Payne, G.S. Composite synthetic lethal identification of membrane traffic inhibitors. *Proc. Natl. Acad. Sci. USA* **104**, 6235–6240 (2007).
31. Li, C. & Wong, W.H. Model-based analysis of oligonucleotide arrays: expression index computation and outlier detection. *Proc. Natl. Acad. Sci. USA* **98**, 31–36 (2001).
32. Ashburner, M. *et al.* Gene ontology: tool for the unification of biology. The Gene Ontology Consortium. *Nat. Genet.* **25**, 25–29 (2000).
33. Longtine, M.S. *et al.* Additional modules for versatile and economical PCR-based gene deletion and modification in *Saccharomyces cerevisiae*. *Yeast* **14**, 953–961 (1998).
34. Chandrasekaran, S. *et al.* Destabilization of binding to cofactors and SCFMet30 is the rate-limiting regulatory step in degradation of polyubiquitinated Met4. *Mol. Cell* **24**, 689–699 (2006).
35. Feldman, R.M., Correll, C.C., Kaplan, K.B. & Deshaies, R.J. A complex of Cdc4p, Skp1p, and Cdc53p/cullin catalyzes ubiquitination of the phosphorylated CDK inhibitor Sic1p. *Cell* **91**, 221–230 (1997).
36. Petroski, M.D. & Deshaies, R.J. In vitro reconstitution of SCF substrate ubiquitination with purified proteins. *Methods Enzymol.* **398**, 143–158 (2005).
37. Booher, K.R. & Kaiser, P. A PCR-based strategy to generate yeast strains expressing endogenous levels of amino-terminal epitope-tagged proteins. *Biotechnol. J.* **3**, 524–529 (2008).
38. Guerrero, C., Tagwerker, C., Kaiser, P. & Huang, L. An integrated mass spectrometry-based proteomic approach: quantitative analysis of tandem affinity-purified in vivo cross-linked protein complexes (QTAX) to decipher the 26 S proteasome-interacting network. *Mol. Cell. Proteomics* **5**, 366–378 (2006).
39. Tagwerker, C. *et al.* A tandem affinity tag for two-step purification under fully denaturing conditions: application in ubiquitin profiling and protein complex identification combined with in vivo cross-linking. *Mol. Cell. Proteomics* **5**, 737–748 (2006).
40. Meierhofer, D., Wang, X., Huang, L. & Kaiser, P. Quantitative analysis of global ubiquitination in HeLa cells by mass spectrometry. *J. Proteome Res.* **7**, 4566–4576 (2008).

doi:10.1038/nbt.1645